

甘肃北山炭山子东橄榄辉长岩年代学、地球化学特征及其地质意义

余君鹏^{1,2}, 王怀涛², 王玉玺³, 孙新春², 任文秀², 魏海峰², 王晓伟²

(1. 兰州大学, 甘肃兰州 730000; 2. 甘肃省地质调查院, 甘肃兰州 730000; 3. 甘肃省地矿局第三地质勘查院, 甘肃兰州 730050)

摘要: 北山地区是中亚造山带的重要组成部分, 位于北山地区大山头杂岩体西的炭山子东基性岩体是揭示中亚造山带南缘晚古生代构造演化的重要载体。炭山子东橄榄辉长岩 LA-ICP-MS 锆石 U-Pb 年龄为 366.0 ± 2.8 Ma, 代表该岩体的形成年龄。岩石 SiO_2 (47.83% ~ 52.25%)、 K_2O (0.12% ~ 0.45%)、 Na_2O (2.47% ~ 3.19%)、 MgO (5.30% ~ 9.22%) 具由拉斑系列向钙碱性系列演化的特点。岩石轻稀土元素 (LREE) 相对富集 [$(\text{La/Yb})_{\text{N}} = 1.57 \sim 4.12$] , 具 Eu 正异常 ($\delta\text{Eu} = 1.15 \sim 1.41$) , 富集大离子亲石元素 (Rb, Ba, Sr, U, K), 亏损高场强元素 (Nb, Ta, Zr 和 Ti), Nb/La 值为 0.23 ~ 0.46, Hf/Th 值为 0.88 ~ 3.81, $(^{87}\text{Sr}/^{86}\text{Sr})_{\text{i}}$ 值为 0.7048 ~ 0.7049, $\varepsilon\text{Nd}(t)$ 值为 +3.72 ~ +4.30, 指示其形成于活动大陆边缘弧环境。结合区域地质, 认为炭山子东橄榄辉长岩是辉铜山—帐房山蛇绿岩所代表的弧后盆地在向北俯冲消减过程中, 受俯冲流体交代的亏损岩石圈地幔发生部分熔融的产物, 为中亚造山带晚泥盆世地壳垂向生长的直接证据。

关键词: 基性杂岩体; 锆石 U-Pb 年龄; Sr-Nd 同位素; 弧后盆地; 北山

中图分类号: P612; P597

文献标识码: A

文章编号: 1000-6524(2021)02-0202-15

Geochronology and geochemistry of Tanshanzidong olivine-gabbro in Beishan area, Gansu Province, and its geological significance

YU Jun-peng^{1,2}, WANG Huai-tao², WANG Yu-xi³, SUN Xin-chun², REN Wen-xiu², WEI Hai-feng² and WANG Xiao-wei²

(1. Lanzhou University, Lanzhou 730000, China; 2. Geological Survey of Gansu Province, Lanzhou 730000, China;
3. Third Institute of Geology and Mineral Exploration, Bureau of Geology and Mineral Resources of Gansu Province,
Lanzhou 730050, China)

Abstract: The Beishan area is an important part of the Central Asian Orogenic Belt. The Tanshanzidong basic complex located west of the Beishan Dashantou complex is an important carrier to reveal the late Paleozoic tectonic evolution on the southern margin of the Central Asian Orogenic Belt. This paper reports that the Tanshanzidong basic complex was emplaced with the zircon U-Pb age of 366.0 ± 2.8 Ma. The rocks are characterized by SiO_2 (47.83% ~ 52.25%), K_2O (0.12% ~ 0.45%), Na_2O (2.47% ~ 3.19%), MgO (5.30% ~ 9.22%) and the evolution from tholeiitic series to calc-alkaline series. The rocks are enriched in LREE [$(\text{La/Yb})_{\text{N}} = 1.57 \sim 4.12$] with positive Eu anomalies, depleted in Nb, Ta, Zr, Ti and enriched in Rb, Ba, Sr, U, K, with the data $\text{Nb/La} = 0.23 \sim 0.46$, $\text{Hf/Th} = 0.88 \sim 3.81$, $(^{87}\text{Sr}/^{86}\text{Sr})_{\text{i}} (0.7048 \sim 0.7049)$ and $\varepsilon\text{Nd}(t)$ (+3.72 ~ +4.30), suggesting that they

收稿日期: 2020-05-20; 接受日期: 2021-01-21; 编辑: 尹淑萍

基金项目: 2020年陇原青年创新创业人才项目(甘组通字[2020]9号); 中国地质调查局项目(12120114014501)

作者简介: 余君鹏(1981-), 男, 博士研究生, 高级工程师, 长期从事区域构造和矿床学研究, E-mail: jpyu12@126.com。

were formed in the arc environment of active continental margin. Based on regional geology, the authors hold that the Tanshanzidong basic complex was the product of partial melting of depleted lithospheric mantle, which was replaced by the subduction fluid during the subduction of the northward subduction of back-arc basin represented by Huitongshan-Zhangfangshan ophiolite. These results provide a direct indication for the vertical growth of the crust caused by the late Devonian crust in the Central Asian Orogenic Belt.

Key words: basic complex; zircon U-Pb dating; Sr-Nd isotope; back-arc basin; Beishan

Fund support: Project of Longyuan Youth Innovation and Entrepreneurship Talent in 2020 ([2020] No. 9); Project of China Geological Survey(12120114014501)

中亚造山带是由微陆块、岛弧、残余洋壳、大陆活动陆缘增生杂岩等组成的世界上最大的古生代增生型造山带(Sengör *et al.*, 1993; Jahn *et al.*, 2000; Xiao *et al.*, 2004, 2010; Windly *et al.*, 2007)。近年来在中亚造山带南缘的东天山和北山地区发现了与基性-超基性岩体有关的多个大中型铜镍硫化物矿床,如坡北、笔架山、黑山等。随着甘肃北山黑山铜镍矿的发现,甘肃北山地区与铜镍硫化物矿床有关的基性-超基性岩引起了广泛关注,并已取得了丰富的研究成果(范育新等,2003;白云来等,2004;王立社等,2008;李丽等,2010a,2010b;邵小阳等,2010;Xie *et al.*, 2012;张新虎等,2012;杨建国等,2012;闫海卿等,2012;徐刚等,2012;谢燮等,2013,2015;王磊等,2013)。但是北山造山带的基性-超基性杂岩体形成时代、岩石成因及其形成的构造动力学背景等重要的科学问题的研究还很薄弱,深入开展北山造山带南缘基性-超基性杂岩的系统研究,探索其岩浆演化过程,论证其源区特征,不仅对了解北山地区地幔源区的性质、演化过程以及地幔演化与地壳形成之间的关系具有重要意义,对完善中亚造山带构造岩浆演化也具有重要的理论和实践意义。

本文通过对北山造山带南缘炭山子东岩体中的橄榄辉长岩进行LA-ICP-MS锆石U-Pb测年和主量、微量元素与Sr-Nd同位素的研究,揭示了岩体成因及其形成的大地构造背景,为北山造山带构造岩浆演化的深入研究提供了重要的地质依据。

1 区域地质背景

北山造山带地处哈萨克斯坦、塔里木、西伯利亚三大板块交汇部位,隶属于中亚造山带南缘,经历了早古生代至早中生代长期的多阶段、复杂的俯冲-拼贴历史(Xiao *et al.*, 2010; Song *et al.*, 2013a,

2013b; Tian *et al.*, 2014; 贺振宇等,2014)。北山造山带是指北至中蒙边界,西邻东天山,东接阿拉善,南以阿尔金和星星峡两大走滑断裂围限的构造楔形区,地质构造较复杂,其大地构造格局和归属也一直存在诸多不同的认识(刘雪亚等,1995;龚全胜等,2002,2003;何世平等,2002;聂凤军等,2002;左国朝等,2003;杨合群等,2010)。北山造山带发育前寒武纪结晶基底,被上覆的古生代地层不整合覆盖,出露地层主要包括寒武系-志留系浅海碎屑岩和火山岩、泥盆系-石炭系海相碎屑岩-碳酸盐岩和岛弧火山岩(安山岩、流纹岩和少量玄武岩)、二叠系浅海相碎屑岩和枕状玄武岩(颉炜等,2013)。北山地区构造岩浆活动十分强烈,侵入岩以花岗岩类最为发育,基性-超基性岩次之,不同规模和走向的断裂构造极为发育,主干断裂带呈近EW向和NEE展布。北山地区许多基性-超基性岩体被认为是弧后盆地型蛇绿岩混杂岩或洋壳型蛇绿混杂岩(于福生等,2000;何世平等,2002;王立社等,2007;张元元等,2008;杨合群等,2010;郑荣国等,2012;武鹏等,2012);而分布在北山南带的一些基性-超基性杂岩体被认为是一种大陆裂谷型的岩浆岩建造(龚全胜等,2003;白云来等,2004;何世平等,2005;杨建国等,2012;王磊等,2013;谢燮等,2015),且区域上已经发现了黑山中型铜镍矿及红柳沟、怪石山、拾金滩、三个井等铜镍矿化岩体,均与基性-超基性岩有关,显示出较好的找矿前景。

大山头杂岩体是甘肃北山地区一个较大的基性-超基性杂岩体,位于红柳河-玉石山-牛圈子蛇绿混杂岩带南缘,黑山-碱泉子深大断裂带北侧,呈NE向凸镜状分布,长约24 km,宽约4 km。杂岩体北部与蓟县纪平头山组白云岩、大理岩呈断层接触,东部侵入于早中奥陶世罗雅楚山组变长石石英砂岩中,南部被早石炭世石英闪长岩侵入破坏,西部被第四系覆盖。大山头杂岩体由红柳沟岩体、炭山子东岩体

和庙庙井岩体等组成(图1)。红柳沟岩体位于大山头岩体东北部,以辉长岩为主,分异出的基性-超基性岩体多呈小岩株和岩脉产出,岩性主要有橄榄角闪苏长岩、橄榄辉长苏长岩、辉石岩、二辉橄榄岩、方辉橄榄岩、辉橄榄岩、纯橄岩等,锆石U-Pb年龄396.7±3.8 Ma(谢燮等,2015)指示其形成于早泥盆世。庙庙井岩体位于大山头岩体东南部,呈透镜状产出,超基性岩主要发育在岩体西部且规模较小,岩性主要为橄榄辉长岩、辉石橄榄岩、橄榄辉石岩等(图2a)。

辉石岩、橄榄辉石岩、辉石橄榄岩、辉长岩等;晚期以角闪辉长岩、闪长岩为主,辉长岩锆石U-Pb年龄374.3±3 Ma(王磊等,2015)指示其形成于晚泥盆世。炭山子东岩体位于大山头杂岩体西南部,出露面积约15 km²,岩性以中细角闪辉长岩和辉长岩为主,在辉长岩中见有少量堆晶辉长岩,向上渐变为细粒辉长岩;分异的基性-超基性岩体面积较小,岩性主要为橄榄辉长岩、辉石橄榄岩、辉长岩等(图2a)。

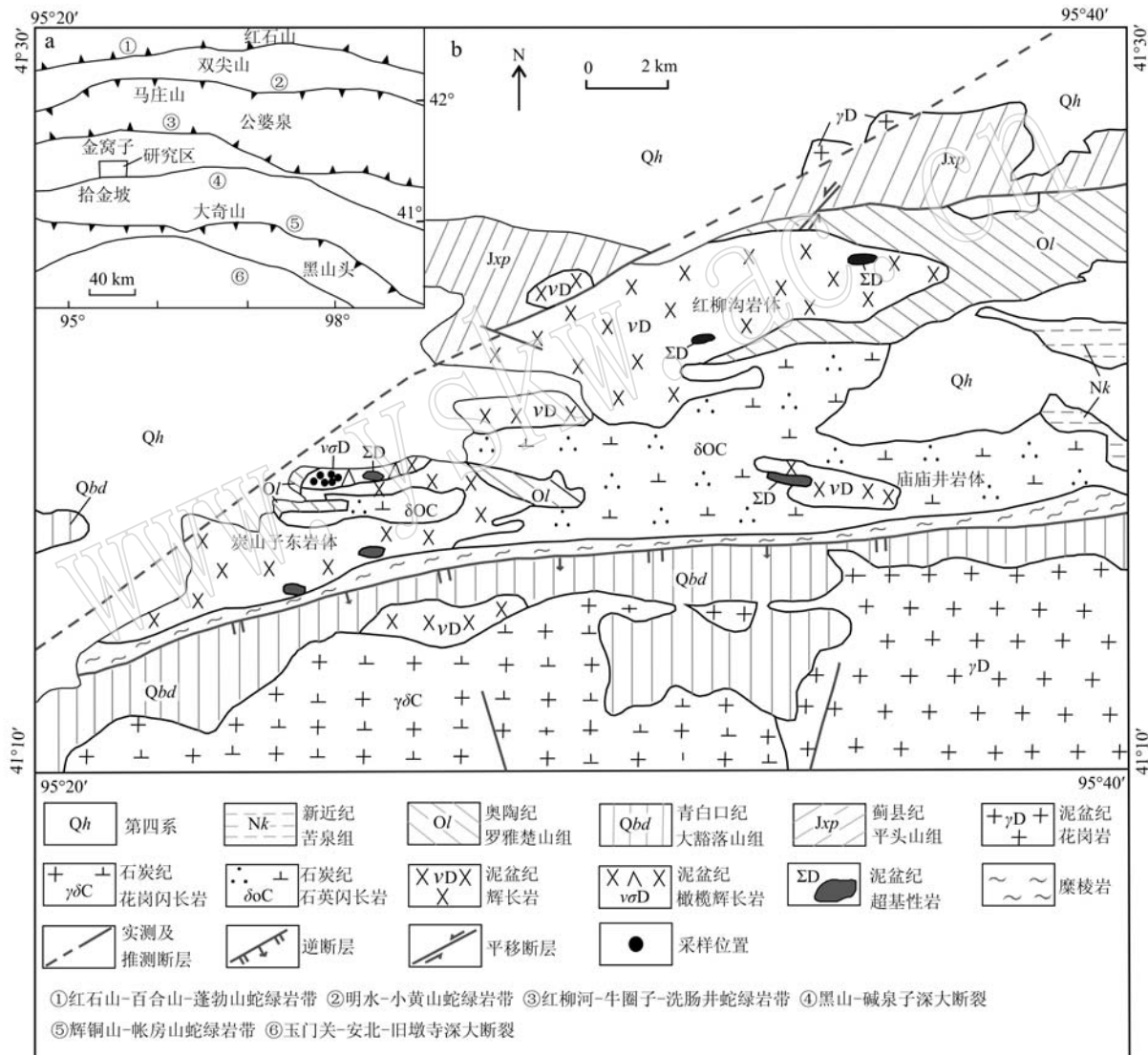


图1 甘肃北山地区构造分区简图(a, 据聂凤军等, 2002)及大山头基性-超基性杂岩体地质简图(b, 据甘肃省地质调查院, 2017^①)

Fig. 1 Map of tectonic zoning of Beishan area (a, after Nie Fengjun et al., 2002) and geological map of basic-ultrabasic complex of Dashantou in Gansu Province (b, after Geological Survey of Gansu Province, 2017^①)

① 甘肃省地质调查院. 2017. 甘肃北山营毛沱-玉石山地区铁铜金钨多金属矿整装勘查区专项填图与技术应用示范报告.

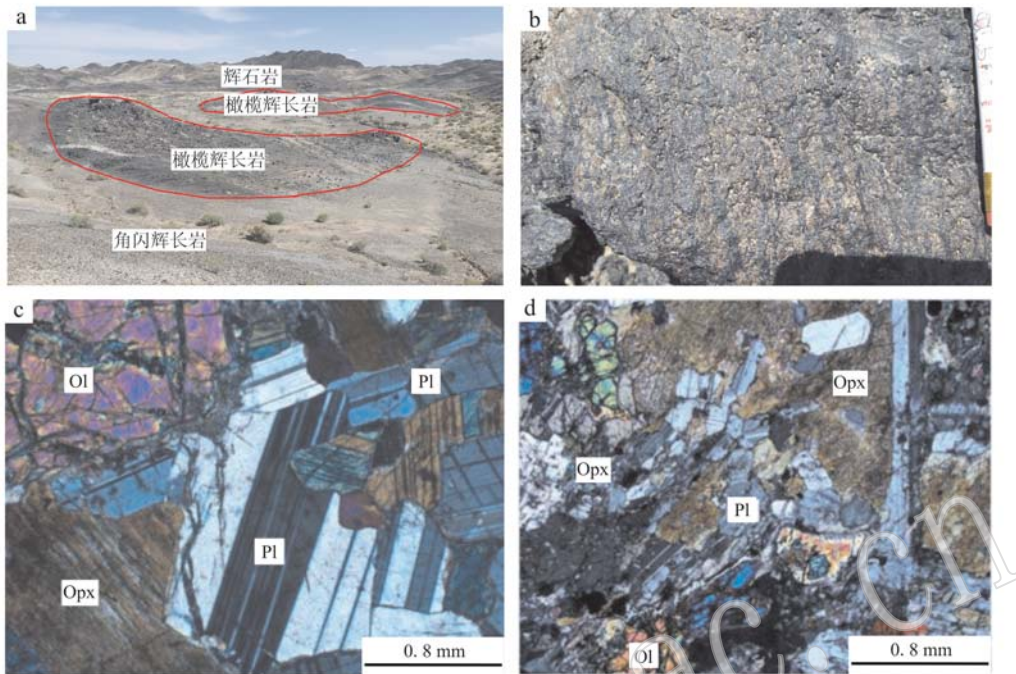


图 2 炭山子东橄榄辉长岩野外露头(a、b)和正交偏光显微特征(c、d)

Fig. 2 Field photos of outcrops (a, b) and photomicrographs under crossed nicols (c, d) of the olivine gabbro of Tanshanzidong

Ol—橄榄石; Opx—斜方辉石; Pl—斜长石
Ol—olivine; Opx—orthopyroxene; Pl—plagioclase

2 岩石学特征

采集炭山子东岩体中的橄榄辉长岩进行分析测试(图 2a)。橄榄辉长岩呈深灰色(图 2b),具细粒柱状结构,块状构造。镜下特征显示(图 2c、2d):橄榄石(15%,体积分数)近浑圆粒状,粒度多在0.6~2.0 mm之间,沿网环状裂理及边缘有较多纤维蛇纹石集合体及少量细小针状纤闪石、细小碳酸盐集合体、磁铁矿等;斜长石(55%)呈板状、宽板状,粒度多在0.5 mm×0.9 mm~2.0 mm×3.0 mm之间,可见细密聚片双晶,An≈65,以拉长石为主,其中粒度大的斜长石可见包裹粒度较小的辉石;斜方辉石(25%)近短柱状、柱状,近垂直的两组解理,沿边缘或解理被少量针状、纤状透闪石、细小碳酸盐集合体、不透明金属矿物等交代,少数被大量纤闪石等蚀变物取代,纤闪石呈针状、纤状较致密排布集合体状,其中不均匀分布少量碳酸盐集合体、微量绿泥石、不透明金属矿物等;副矿物有磷灰石、榍石及不透明金属矿物。

3 分析方法

样品取自炭山子东岩体,采集1件锆石U-Pb测年样和6件岩石地球化学分析样,岩性均为橄榄辉长岩,具体采样位置见图1。

3.1 LA-ICP-MS 测年

锆石的分选由河北省廊坊地质调查研究所实验室完成。样品经常规粉碎至100目左右,采用重液法和电磁法进行分选,再通过双目镜手工精选无包裹体、无裂纹和透明度高的晶形完好的单颗粒锆石作为测定对象。锆石CL(阴极发光)研究及LA-ICP-MS锆石U-Pb测定在中国地质大学(武汉)地质过程与矿产资源国家重点实验室完成。实验采用电感耦合等离子体质谱仪(Agilent7500a)和激光剥蚀系统(GeoLas 2005)联机进行,激光束斑直径为32 μm,剥蚀深度为20~40 μm,采用He作为剥蚀物质的载气。锆石年龄测定采用国际标准锆石91500($^{206}\text{Pb}/^{238}\text{U}$ 年龄为1 065.4±0.6 Ma,Wiedenbeck *et al.*, 1995)作为校正外标,元素含量采用NIST SRM 612作

为外标,²⁹Si作为内标进行校正。采样方式为单点剥蚀,每完成5个测点的样品测定,加测标样1次。具体分析流程、方法见参考文献(Yuan et al., 2004)。对分析数据的离线处理运用ICPMS-DataCal(V8.0)软件计算得出,并利用Isoplot-ver3进行锆石年龄谱和图绘制和年龄权重计算。

3.2 主量、微量元素分析

样品主、微量元素分析测试在广州澳实矿物实验室(ALS Minerals-ALS Chemex)完成,主量元素采用X射线荧光光谱(ME-XRF26d)分析,分析精度优于5%;微量元素采用电感耦合离子质谱仪(ICP-MS)分析,分析过程分别用高温高压四酸消解和硼酸锂熔融法,分析精度高于10%;亚铁分析采用Fe-VOL05的方法,先用酸消解,再用重铬酸钾滴定测量。

3.3 Sr-Nd同位素分析

Sr-Nd同位素在中国科学院广州地球化学研究

所同位素超净实验室进行,所用仪器为Micromass IsoProbeTM型MC-ICP-MS,所有样品的¹⁴³Nd/¹⁴⁴Nd和⁸⁷Sr/⁸⁶Sr统一采用¹⁴⁶Nd/¹⁴⁴Nd=0.7219和⁸⁶Sr/⁸⁸Sr=0.1194分别进行标准化,具体的实验流程参见韦刚健等(2002)和梁细荣等(2003)。

4 同位素年代学

4.1 锆石特征

锆石呈灰白色-灰色,自形程度较好,颗粒大小约为80~300μm,锆石中U,Th含量较低,个别锆石含量较高,Th/U值为0.41~2.99(表1),仅TSD-23为0.09,TSD-27为0.26,且U,Th含量呈现出较好的正相关关系,在阴极发光影像图上(图3)锆石具明显的岩浆振荡环带结构,表现出典型的岩浆锆石特征。

表1 炭山子东橄榄辉长岩中的LA-ICP-MS锆石U-Pb分析数据
Table 1 Zircon LA-ICP-MS U-Pb data of olivine gabbro from Tanshanzidong

| 点号 | $w_B/10^{-6}$ | | | | 同位素比值 | | | | 年龄/Ma | | | |
|---------|---------------|-------------------|------------------|-------------------------------------|-------------------------------------|--------|-------------------------------------|--------|-------------------------------------|----|-------------------------------------|----|
| | Pb | ²³² Th | ²³⁸ U | ²³² Th/ ²³⁸ U | ²⁰⁷ Pb/ ²³⁵ U | 1σ | ²⁰⁶ Pb/ ²³⁸ U | 1σ | ²⁰⁷ Pb/ ²³⁵ U | 1σ | ²⁰⁶ Pb/ ²³⁸ U | 1σ |
| TSD-1 | 12.95 | 85.47 | 173.06 | 0.49 | 0.4089 | 0.0144 | 0.0575 | 0.0006 | 348 | 10 | 360 | 4 |
| TSD-2 | 13.93 | 123.01 | 126.07 | 0.98 | 0.4035 | 0.0150 | 0.0576 | 0.0007 | 344 | 11 | 361 | 4 |
| TSD-3 | 6.16 | 48.74 | 65.39 | 0.75 | 0.3929 | 0.0266 | 0.0565 | 0.0008 | 337 | 19 | 354 | 5 |
| TSD-4 | 16.41 | 152.39 | 124.02 | 1.23 | 0.4205 | 0.0164 | 0.0572 | 0.0006 | 356 | 12 | 358 | 4 |
| TSD-5 | 12.31 | 116.65 | 99.25 | 1.18 | 0.4062 | 0.0205 | 0.0569 | 0.0007 | 346 | 15 | 357 | 4 |
| TSD-6 | 21.08 | 200.87 | 161.24 | 1.25 | 0.3928 | 0.0131 | 0.0580 | 0.0006 | 336 | 10 | 363 | 4 |
| TSD-7 | 7.11 | 55.25 | 76.97 | 0.72 | 0.4347 | 0.0194 | 0.0590 | 0.0009 | 367 | 14 | 369 | 6 |
| TSD-8 | 8.03 | 64.36 | 76.16 | 0.85 | 0.3978 | 0.0182 | 0.0595 | 0.0006 | 340 | 13 | 372 | 4 |
| TSD-9 | 113.71 | 1016.49 | 679.50 | 1.50 | 0.4193 | 0.0089 | 0.0598 | 0.0005 | 356 | 6 | 374 | 3 |
| TSD-10 | 34.53 | 285.81 | 314.43 | 0.91 | 0.4185 | 0.0121 | 0.0598 | 0.0006 | 355 | 9 | 375 | 4 |
| TSD-11 | 158.34 | 1598.57 | 534.51 | 2.99 | 0.4257 | 0.0094 | 0.0597 | 0.0005 | 360 | 7 | 374 | 3 |
| TSD-12 | 26.18 | 255.90 | 185.11 | 1.38 | 0.4365 | 0.0147 | 0.0586 | 0.0008 | 368 | 10 | 367 | 5 |
| TSD-13 | 33.99 | 316.29 | 275.27 | 1.15 | 0.3994 | 0.0118 | 0.0578 | 0.0005 | 341 | 9 | 362 | 3 |
| TSD-14 | 17.96 | 160.26 | 126.29 | 1.27 | 0.4353 | 0.0167 | 0.0577 | 0.0006 | 367 | 12 | 362 | 4 |
| TSD-15 | 7.40 | 56.97 | 83.63 | 0.68 | 0.4161 | 0.0213 | 0.0581 | 0.0007 | 353 | 15 | 364 | 4 |
| TSD-16 | 11.37 | 106.71 | 96.55 | 1.11 | 0.4291 | 0.0179 | 0.0582 | 0.0007 | 363 | 13 | 365 | 4 |
| TSD-17 | 11.55 | 101.11 | 94.36 | 1.07 | 0.4476 | 0.0169 | 0.0594 | 0.0008 | 376 | 12 | 372 | 5 |
| TSD-18 | 18.17 | 133.48 | 205.84 | 0.65 | 0.4174 | 0.0128 | 0.0588 | 0.0006 | 354 | 9 | 369 | 3 |
| TSD-19 | 14.45 | 86.76 | 212.86 | 0.41 | 0.4450 | 0.0133 | 0.0585 | 0.0006 | 374 | 9 | 367 | 4 |
| TSD-20 | 61.28 | 582.84 | 398.55 | 1.46 | 0.4326 | 0.0109 | 0.0596 | 0.0006 | 365 | 8 | 373 | 4 |
| TSD-21 | 18.91 | 155.71 | 188.39 | 0.83 | 0.3964 | 0.0110 | 0.0570 | 0.0006 | 339 | 8 | 358 | 4 |
| TSD-22 | 35.93 | 307.90 | 323.43 | 0.95 | 0.4216 | 0.0115 | 0.0593 | 0.0005 | 357 | 8 | 371 | 3 |
| TSD-23 | 14.43 | 30.90 | 334.65 | 0.09 | 0.4174 | 0.0098 | 0.0585 | 0.0005 | 354 | 7 | 367 | 3 |
| TSD-24* | 10.87 | 14.47 | 237.92 | 0.06 | 0.4725 | 0.0151 | 0.0639 | 0.0006 | 393 | 10 | 399 | 4 |
| TSD-25 | 23.02 | 212.36 | 181.55 | 1.17 | 0.4217 | 0.0129 | 0.0581 | 0.0005 | 357 | 9 | 363 | 3 |
| TSD-26 | 13.94 | 92.58 | 166.85 | 0.55 | 0.4508 | 0.0129 | 0.0601 | 0.0007 | 378 | 9 | 376 | 4 |
| TSD-27 | 24.20 | 108.80 | 425.66 | 0.26 | 0.4281 | 0.0122 | 0.0556 | 0.0006 | 362 | 9 | 349 | 4 |

注:表中标*的不参与²⁰⁶Pb/²³⁸U年龄的加权平均。

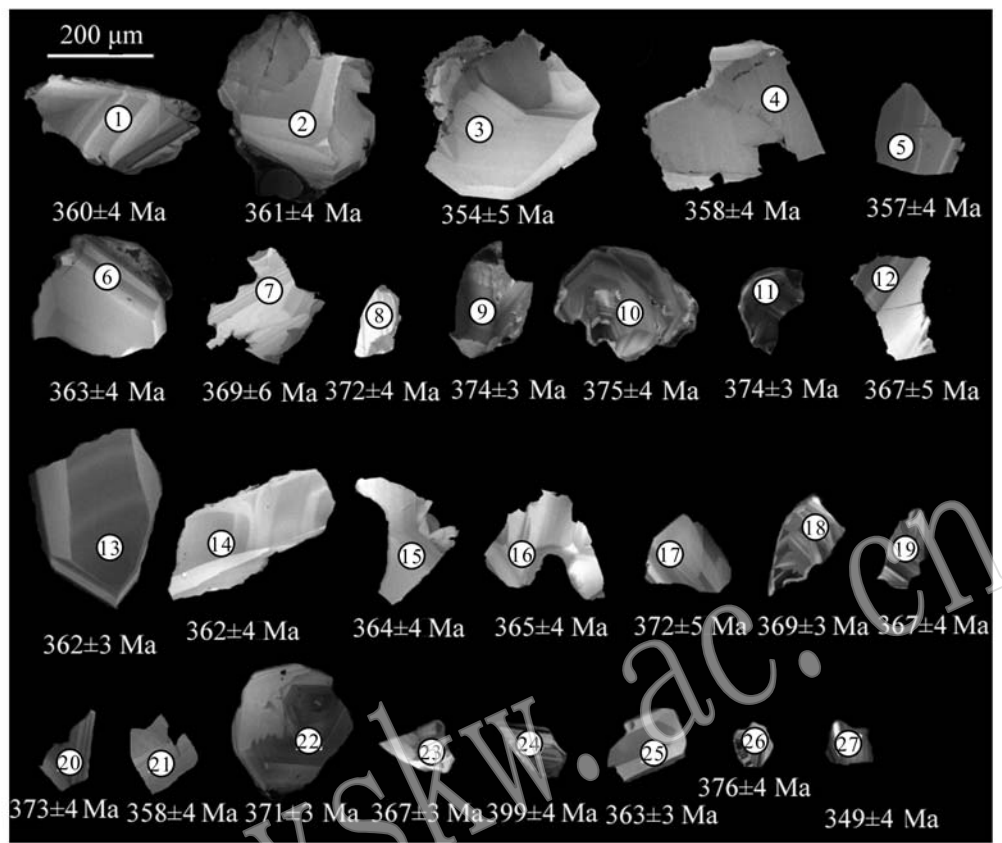


图3 炭山子东橄榄辉长岩锆石CL和LA-ICP-MS测点位置图

Fig. 3 CL images and dating spots of zircons of olivine gabbro from Tanshanzidong

4.2 LA-ICP-MS 锆石 U-Pb 定年结果

本次实验共选取 27 个锆石, 共 27 个测点, 打点位置边部和核部均有分布。在锆石 LA-ICP-MS U-Pb 年龄谐和图上, 除点号 TSD1-24 的 $^{206}\text{Pb}/^{238}\text{U}$ 年龄值明显偏老、可能为捕获锆石外, 其余 26 个锆石分析点的 $^{206}\text{Pb}/^{238}\text{U}$ 年龄介于 376~349 Ma, 锆石颗粒样品都投影在谐和曲线上或谐和曲线上附近, 表明这些颗粒形成后 U-Pb 同位素体系是封闭的, 基本没有 U 或 Pb 同位素的丢失或加入, 其加权平均值为 366.0 ± 2.8 Ma (95% conf., MSWD = 3.4, 1σ) (图 4), 可信度高, 可以解释为橄榄辉长岩的结晶时间, 指示该岩体形成时代为中晚泥盆世。

5 岩体地球化学特征

5.1 主量元素特征

从表 2 可知, 炭山子东橄榄辉长岩具相对较低的 SiO_2 (47.83%~50.25%) 含量, 相对较高的 Al_2O_3 (17.37%~22.34%)、 MgO (5.30%~9.22%, $\text{Mg}^{\#}$ 为

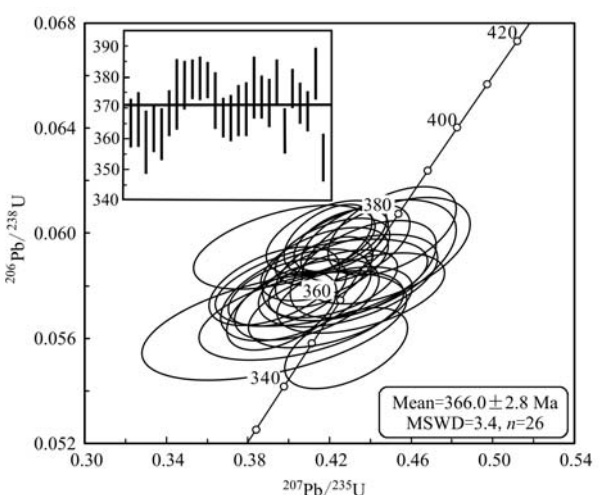


图4 炭山子东橄榄辉长岩锆石 U-Pb 年龄谐和图

Fig. 4 Concordia diagram of zircon U-Pb data of olivine gabbro from Tanshanzidong

67~74) 和 CaO (9.64%~12.65%) 含量, 富钠贫钾 ($\text{Na}_2\text{O} = 2.47\% \sim 3.19\%$, $\text{K}_2\text{O} = 0.12\% \sim 0.45\%$), 以及较低的 TiO_2 (0.35%~0.63%) 和 Fe_2O_3 (5.12%~

表2 炭山子东橄榄辉长岩主量元素($w_B/\%$)、微量元素($w_B/10^{-6}$)地球化学分析结果

Table 2 Major ($w_B/\%$) and trace element ($w_B/10^{-6}$) compositions of the olivine gabbro from Tanshanzidong

| 样号 | B505 | B506 | B507 | B508 | B509 | B510 |
|---------------------------------|--------|--------|--------|--------|--------|--------|
| SiO ₂ | 49.36 | 49.89 | 47.83 | 50.25 | 49.91 | 49.84 |
| Al ₂ O ₃ | 17.46 | 17.61 | 20.60 | 22.34 | 17.37 | 22.04 |
| FeO | 6.17 | 5.84 | 5.97 | 4.12 | 5.01 | 4.03 |
| TFe ₂ O ₃ | 7.65 | 7.08 | 7.61 | 5.16 | 6.25 | 5.12 |
| CaO | 11.65 | 12.15 | 9.64 | 12.25 | 12.65 | 11.45 |
| MgO | 9.22 | 9.16 | 8.38 | 5.30 | 9.09 | 5.46 |
| K ₂ O | 0.18 | 0.16 | 0.20 | 0.16 | 0.12 | 0.45 |
| Na ₂ O | 2.62 | 2.69 | 3.10 | 3.19 | 2.47 | 3.06 |
| TiO ₂ | 0.63 | 0.55 | 0.49 | 0.55 | 0.35 | 0.49 |
| P ₂ O ₅ | 0.05 | 0.06 | 0.10 | 0.05 | 0.01 | 0.12 |
| MnO | 0.13 | 0.12 | 0.11 | 0.08 | 0.11 | 0.09 |
| LOI | 0.51 | 0.57 | 1.74 | 0.49 | 1.22 | 1.24 |
| Total | 105.63 | 105.88 | 105.77 | 103.94 | 104.60 | 103.39 |
| Mg [#] | 71 | 72 | 69 | 67 | 74 | 68 |
| Cu | 58.04 | 50.27 | 60.31 | 38.28 | 60.17 | 20.06 |
| Ni | 91.89 | 114.92 | 87.03 | 67.12 | 132.20 | 67.03 |
| Co | 39.01 | 37.12 | 40.05 | 24.13 | 33.11 | 22.06 |
| Rb | 4.11 | 3.23 | 6.71 | 3.12 | 2.73 | 22.44 |
| Sr | 276.13 | 292.22 | 321.41 | 374.05 | 277.34 | 371.02 |
| Ba | 52.72 | 47.53 | 57.80 | 57.73 | 33.12 | 77.80 |
| V | 163.22 | 161.01 | 57.23 | 115.31 | 137.02 | 109.11 |
| Sc | 26.88 | 28.02 | 6.01 | 14.97 | 30.32 | 13.04 |
| Nb | 1.70 | 1.22 | 1.71 | 1.33 | 0.51 | 1.62 |
| Ta | 0.20 | 0.09 | 0.10 | 0.09 | 0.11 | 0.13 |
| Zr | 48.87 | 38.12 | 54.23 | 38.11 | 15.04 | 46.96 |
| Hf | 1.41 | 1.10 | 1.31 | 1.12 | 0.60 | 1.21 |
| Ga | 14.76 | 14.72 | 15.48 | 17.09 | 13.71 | 17.47 |
| U | 0.08 | 0.06 | 0.78 | 0.07 | 0.21 | 0.20 |
| Th | 0.37 | 0.30 | 0.56 | 0.30 | 0.68 | 0.36 |
| Y | 15.92 | 13.31 | 8.50 | 11.01 | 11.42 | 13.31 |
| La | 3.70 | 3.13 | 4.42 | 3.41 | 2.23 | 5.01 |
| Ce | 9.03 | 7.62 | 10.01 | 8.02 | 5.41 | 10.50 |
| Pr | 1.32 | 1.09 | 1.24 | 1.05 | 0.73 | 1.53 |
| Nd | 6.31 | 5.50 | 5.62 | 4.81 | 3.82 | 7.10 |
| Sm | 1.91 | 1.57 | 1.33 | 1.34 | 1.23 | 1.81 |
| Eu | 0.89 | 0.83 | 0.76 | 0.85 | 0.66 | 0.89 |
| Gd | 2.37 | 1.98 | 1.36 | 1.56 | 1.56 | 2.19 |
| Tb | 0.42 | 0.36 | 0.23 | 0.30 | 0.30 | 0.36 |
| Dy | 2.79 | 2.28 | 1.42 | 1.87 | 1.88 | 2.21 |
| Ho | 0.58 | 0.47 | 0.29 | 0.36 | 0.40 | 0.45 |
| Er | 1.73 | 1.39 | 0.82 | 1.12 | 1.12 | 1.36 |
| Tm | 0.24 | 0.20 | 0.12 | 0.16 | 0.17 | 0.19 |
| Yb | 1.50 | 1.26 | 0.77 | 0.99 | 1.02 | 1.21 |
| Lu | 0.22 | 0.18 | 0.12 | 0.14 | 0.14 | 0.18 |
| Σ REE | 33.01 | 27.86 | 28.51 | 25.98 | 20.67 | 34.99 |
| LREE | 23.16 | 19.74 | 23.38 | 19.48 | 14.08 | 26.84 |
| HREE | 9.85 | 8.12 | 5.13 | 6.50 | 6.59 | 8.15 |
| LREE/HREE | 2.35 | 2.43 | 4.56 | 3.00 | 2.14 | 3.29 |
| (La/Yb) _N | 1.77 | 1.78 | 4.12 | 2.47 | 1.57 | 2.97 |
| (Nb/La) _N | 0.44 | 0.38 | 0.37 | 0.38 | 0.22 | 0.31 |
| δ Eu | 1.15 | 1.22 | 1.41 | 1.39 | 1.22 | 1.20 |

注: δ Eu = Eu_N / (Eu_N × Gd_N)^{1/2}。

7.65%)含量的地球化学特征。在 TAS 图解中样品落在辉长岩区, 在 K₂O-SiO₂ 相关图解上样品落在低钾拉斑系列(图 5)。

5.2 微量元素特征

岩石稀土元素总量偏低, Σ REE 为 $20.67 \times 10^{-6} \sim 34.99 \times 10^{-6}$, 其中 LREE 为 $14.08 \times 10^{-6} \sim 26.84 \times 10^{-6}$, HREE 为 $5.13 \times 10^{-6} \sim 9.85 \times 10^{-6}$, LREE/HREE 为 $2.35 \sim 4.56$, 与黑山、红柳沟、怪石山岩体稀土元素特征相近(李丽等, 2010b; Xie et al., 2012; 谢燮等, 2015)。球粒陨石标准化稀土元素配分模式图为略微右倾型, 且重稀土元素配分曲线相对平坦(图 6a), (La/Yb)_N 为 $1.57 \sim 4.12$, LREE 略富集; 具明显的 δ Eu 正异常, δ Eu 为 $1.15 \sim 1.41$, 可能与斜长石的堆晶有关。原始地幔标准化微量元素蛛网图显示(图 6b), 橄榄辉长岩富集大离子亲石元素 Rb、Ba、Sr、U、K, 且富集程度明显不同, 亏损高场强元素 Nb、Ta、Zr、P、Ti。

5.3 Sr、Nd 同位素特征

由表 3 可见, 炭山子东橄榄辉长岩样品 $^{87}\text{Sr}/^{86}\text{Sr}$ 介于 $0.7050 \sim 0.7052$ 之间, 初始锶($^{87}\text{Sr}/^{86}\text{Sr}$)_i 值为 $0.7048 \sim 0.7049$, $^{147}\text{Sm}/^{144}\text{Nd}$ 值为 $0.1430 \sim 0.1829$, $^{143}\text{Nd}/^{144}\text{Nd}$ 值为 $0.5127 \sim 0.5128$, $\varepsilon\text{Nd}(t)$ 为 $+3.72 \sim +4.30$, 二阶段法计算获得的 Nd 模式年龄 t_{DM2} 为 $1697 \sim 964$ Ma。

6 讨论

6.1 岩石成因

炭山子东橄榄辉长岩 Sr 同位素初始值($0.7048 \sim 0.7049$)以及正的 $\varepsilon\text{Nd}(t)$ 值($+3.72 \sim +4.30$)与坡北岩体接近(姜常义等, 2006)。在 $\varepsilon\text{Nd}(t)$ - $^{87}\text{Sr}/^{86}\text{Sr}$ 图解上样品落入第一象限(图 7), 显示该岩体源自亏损地幔。橄榄辉长岩的微量元素原始地幔标准化蛛网图和稀土元素球粒陨石标准化配分模式图(图 6)与源自亏损软流圈地幔的 N-MORB 具有明显的差异。

炭山子东橄榄辉长岩富集轻稀土元素和 Rb、Ba、Sr 等大离子亲石元素, 亏损 Nb、Ta、Ti、Zr、P 等高场强元素, Ta/La 值($0.02 \sim 0.05$, 平均 0.03)低于原始地幔 Ta/La 值(0.06) (Wood et al., 1979), 说明成岩过程中可能存在地壳物质的混染。样品的 Th($\leq 0.68 \times 10^{-6}$)、Ba($\leq 77.80 \times 10^{-6}$)、Rb($\leq 22.44 \times$

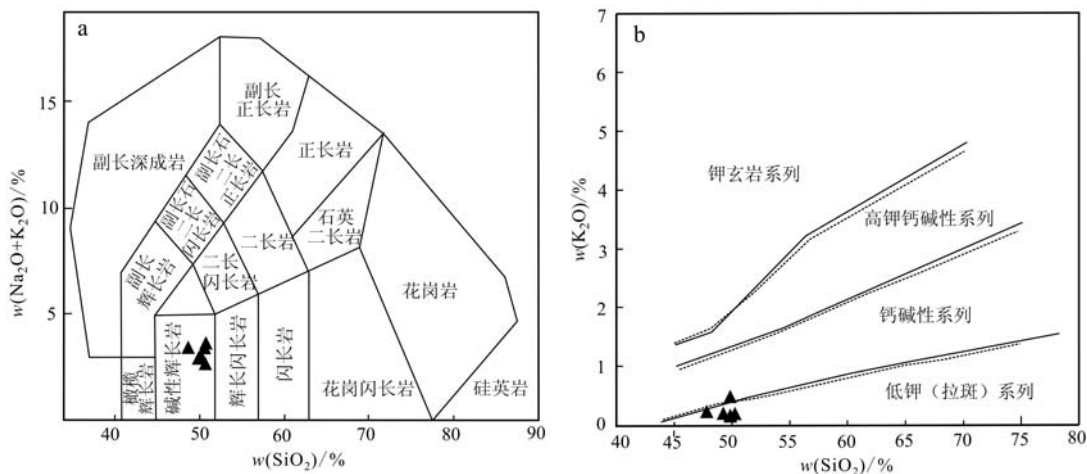


图 5 炭山子东橄榄辉长岩 TAS 图解(a, 据 Wilson, 1989) 和 K_2O-SiO_2 图解(b, 据 Rickwood, 1989)

Fig. 5 TAS (a, after Wilson, 1989) and K₂O-SiO₂ (b, after Rickwood, 1989) diagrams of the olivine gabbro from Tanshanzidong

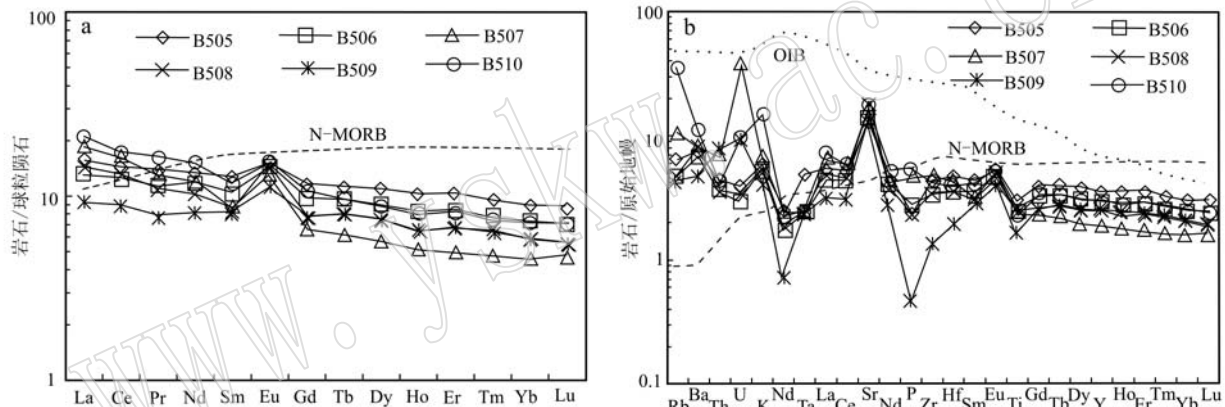


图 6 炭山子东橄榄辉长岩球粒陨石标准化稀土元素配分图(a)和微量元素原始地幔标准化蛛网图(b)(标准化值据 Sun and Mc Donough, 1989)

Fig. 6 Primitive normalized chondrite-normalized REE patterns (a) and trace element spider diagram (b) (normalized values after Sun and McDonough, 1989)

10^{-6})含量明显低于大陆地壳平均含量(5.6×10^{-6} 、 390×10^{-6} 、 58×10^{-6}) (Sun and McDonough, 1989), Yb 值(0.77×10^{-6} ~ 1.50×10^{-6}) 小于 5×10^{-6} , Ta 值(0.09×10^{-6} ~ 0.20×10^{-6}) 小于 1×10^{-6} , Ta/Yb 值(0.08~0.13) 小于 0.5, 指示岩浆源区存在与俯冲带有关的组分(Condie, 1989)。 $(Nb/La)_N$ 值为 $0.22 \sim 0.44$, 远小于 1, 暗示地幔源区可能含有部分熔融交代或者是被消减板片脱水的地幔楔物质(Elliott *et al.*, 1997; Wilson, 1989)。 $La/Ba - La/Nb$ 和 $(Hf/Sr)_N - (Ta/La)_N$ 图解也反映了源区为被俯冲流体交代改造的地幔楔物质(图 8)。岩体正常的($^{87}Sr/^{86}Sr$)_i 值(0.7048~0.7049) 及正的 $\varepsilon Nd(t)$ 值(+3.72~+4.30)、 La/Sm (1.81~3.23) 均小于 5, 同样表明地

壳混染程度不大。这些地球化学特征表明橄榄辉长岩的岩浆源区受到俯冲流体的交代作用，而不是岩浆作用过程中大陆地壳物质混染的结果。

炭山子东橄榄辉长岩富集 Rb、Ba、Sr、K、U 等大离子亲石元素, 亏损 Nb、Ta、Sr、Zr、Hf、Ti 等高场强元素, 显示出典型的火山弧火成岩的地球化学特征。Nb/La 值(0.23~0.46, 平均 0.36) 接近典型岛弧岩浆岩的 Nb/La 值(约 0.3), 远低于 OIB 的 Nb/La 值(1.30); Hf/Th 值(0.88~3.81, 平均 2.97) 与岛弧玄武岩(Hf/Th<8) 相类似(Condie, 1989)。在 Hf/3-Th-Nb/16 图解上所有样品均落入岛弧区(图 9), 样品具有由拉斑系列向钙碱性系列演化的特点, 在 Th/Yb-Ta/Yb 图解中大部分样品落入活动大陆边缘

表3 炭山子东橄榄辉长岩Sr、Nd同位素数据

Table 3 Sr, Nd isotopic data for the olivine gabbro from Tanshanzidong

| 样号 | B505 | B506 | B507 |
|---------------------------------------|-----------|-----------|-----------|
| 年龄/Ma | 366 | 366 | 366 |
| Rb | 4.11 | 3.23 | 6.71 |
| Sr | 276.13 | 292.22 | 321.41 |
| $^{87}\text{Rb}/^{86}\text{Sr}$ | 0.043 0 | 0.032 0 | 0.060 4 |
| $^{87}\text{Sr}/^{86}\text{Sr}$ | 0.705 0 | 0.705 1 | 0.705 2 |
| $\pm 2\sigma$ | 0.000 009 | 0.000 008 | 0.000 009 |
| $(^{87}\text{Sr}/^{86}\text{Sr})_i$ | 0.704 8 | 0.704 9 | 0.704 9 |
| Sm | 1.91 | 1.57 | 1.33 |
| Nd | 6.31 | 5.50 | 5.62 |
| $^{147}\text{Sm}/^{144}\text{Nd}$ | 0.182 9 | 0.172 5 | 0.143 0 |
| $^{143}\text{Nd}/^{144}\text{Nd}$ | 0.512 8 | 0.512 8 | 0.512 7 |
| $\pm 2\sigma$ | 0.000 005 | 0.000 005 | 0.000 006 |
| $(^{143}\text{Nd}/^{144}\text{Nd})_i$ | 0.512 4 | 0.512 4 | 0.512 4 |
| $\varepsilon\text{Nd}(t)$ | 3.81 | 4.30 | 3.72 |
| t_{DM2}/Ma | 1.697 | 1.291 | 964 |

注: $\varepsilon\text{Nd} = [(\text{Nd}^{143}/\text{Nd}^{144})_s / (\text{Nd}^{143}/\text{Nd}^{144})_{\text{CHUR}} - 1] \times 10000$, 其中 s 表示样品, $(^{87}\text{Rb}/^{86}\text{Sr})_{\text{CHUR}} = 0.0847$, $(^{87}\text{Sr}/^{86}\text{Sr})_{\text{CHUR}} = 0.7045$, $(^{143}\text{Nd}/^{144}\text{Nd})_{\text{CHUR}} = 0.512638$, $(^{147}\text{Sm}/^{144}\text{Nd})_{\text{CHUR}} = 0.1966$; $\lambda_{\text{Rb}} = 1.42 \times 10^{-11} \text{ a}^{-1}$, $\lambda_{\text{Sm}} = 6.54 \times 10^{-12} \text{ a}^{-1}$; t 为岩体侵位年龄。

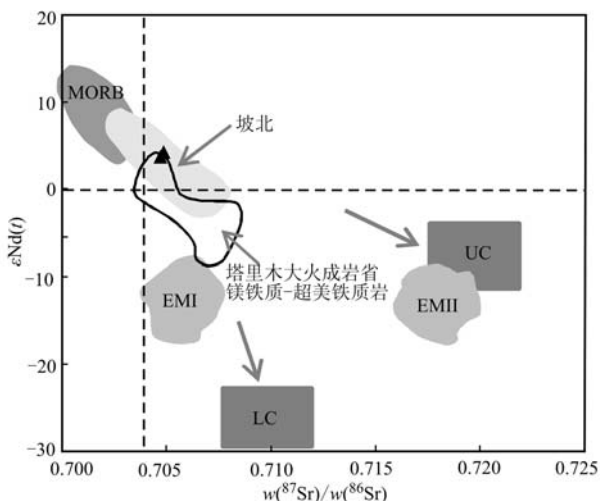


图7 炭山子东橄榄辉长岩 $\varepsilon\text{Nd}(t)$ - $^{87}\text{Sr}/^{86}\text{Sr}$ 图解
(据 Zindler et al., 1986)

Fig. 7 $\varepsilon\text{Nd}(t)$ - $^{87}\text{Sr}/^{86}\text{Sr}$ diagram of the olivine gabbro from Tanshanzidong (after Zindler et al., 1986)

MORB—洋中脊玄武岩; EM I—I型富集地幔; EM II—II型富集地幔; LC—下地壳; UC—上地壳
MORB—mid ocean ridge basalt; EM I—I enrichment mantle; EM II—II enrichment mantle; LC—lower crust; UC—upper crust

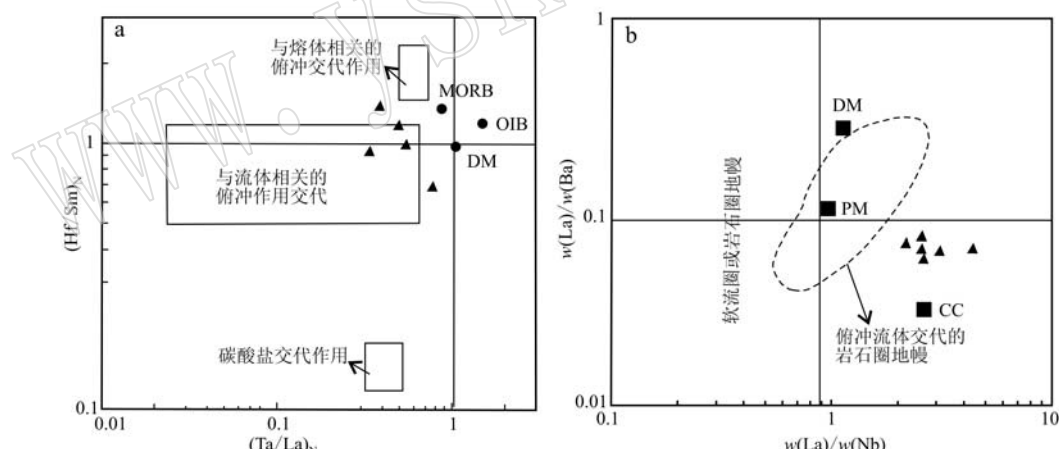


图8 $(\text{Hf}/\text{Sm})_N - (\text{Ta}/\text{La})_N$ 图和 $\text{La}/\text{Ba} - \text{La}/\text{Nb}$ 图解(据 La Flèche et al., 1998)

Fig. 8 $(\text{Hf}/\text{Sm})_N - (\text{Ta}/\text{La})_N$ and $\text{La}/\text{Ba} - \text{La}/\text{Nb}$ diagrams of the olivine gabbro from Tanshanzidong (after La Flèche et al., 1998)

MORB—洋中脊玄武岩; OIB—洋岛型玄武岩; DM—亏损地幔; PM—原始地幔; CC—大陆地壳

MORB—mid ocean ridge basalt; OIB—ocean island basalt; DM—depleted mantle; PM—primitive mantle; CC—continental crust

缘附近(图10)。综上所述,炭山子东橄榄辉长岩应是受俯冲流体交代的亏损岩石圈地幔在活动大陆边缘弧环境下部分熔融的产物。

6.2 大地构造意义

北山地区在经历了中元古代蓟县纪和新元古代青白口纪巨厚的碳酸盐岩及碎屑岩沉积之后,发生了晋宁运动,使前震旦系完全固结形成统一古大陆

克拉通(左国朝等, 1996)。李锦铁等(2006)通过对塔里木盆地北缘和扬子陆块北缘震旦纪地层中火山沉积岩系的分析研究以及天山及毗邻地区蛇绿岩、活动大陆边缘的同位素年代学资料的研究,认为古亚洲洋盆是在震旦纪开始打开的。近年来,中亚造山带北山地区蛇绿岩研究获得了许多高精度的锆石SHRIMP U-Pb 年学资料,如北山月牙山蛇绿岩套中斜

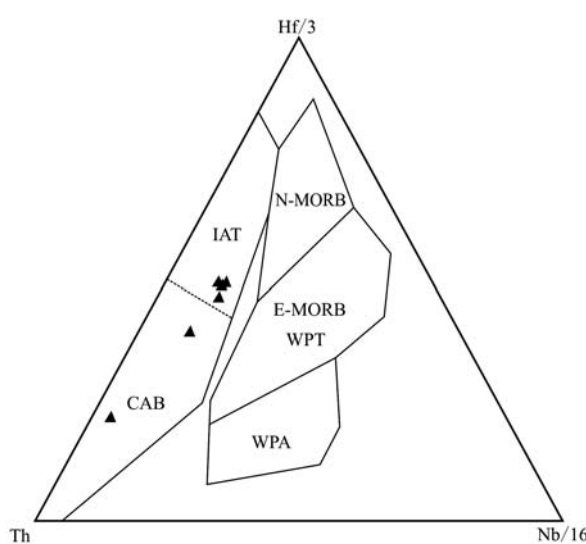


图 9 $\text{Hf}/3 - \text{Th} - \text{Nb}/16$ 构造判别图解(据 Wood *et al.*, 1979)

Fig. 9 $\text{Hf}/3 - \text{Th} - \text{Nb}/16$ diagram (after Wood *et al.*, 1979)

N-MORB—洋中脊玄武岩; E-MORB—富集型洋中脊玄武岩; IAT—岛弧拉斑玄武岩; CAB—钙碱性玄武岩; WPT—板内拉斑玄武岩; WPA—板内碱性玄武岩图
N-MORB—normal mid-ocean ridge basalt; E-MORB—enriched mid-oceanic ridge basalt; IAT—island-arc laporite basalts; CAB—calcium alkaline basalts; WPT—within-plate tholeiites; WPA—alkaline within-plate basalts

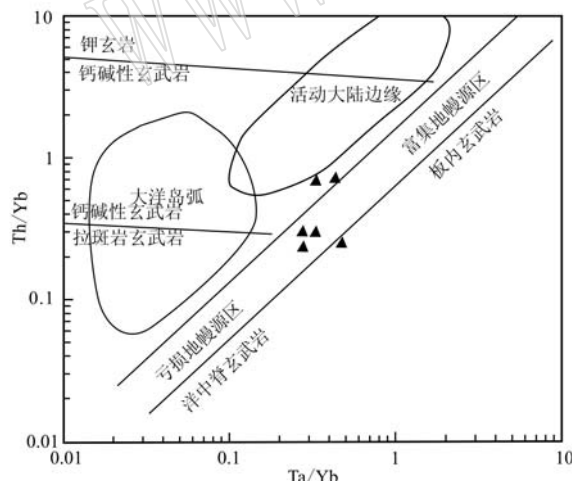


图 10 $\text{Th}/\text{Yb} - \text{Ta}/\text{Yb}$ 构造图解(据 Pearce *et al.*, 1984)
Fig. 10 $\text{Th}/\text{Yb} - \text{Ta}/\text{Yb}$ diagram (after Pearce *et al.*, 1984)

长花岗岩的 SHRIMP 锆石 U-Pb 年龄 536 ± 7 Ma、红柳河蛇绿岩中堆晶辉长岩的 SHRIMP 锆石 U-Pb 年龄 516 ± 7.1 Ma(张元元等, 2008; 侯青叶等, 2012), 指示北山地区红柳河-牛圈子-洗肠井-月牙山古大洋在早寒武世已经形成, 并于志留纪期间洋盆发生

了大规模自南向北的俯冲作用(左国朝等, 1996; 戴霜等, 2003; 何世平等, 2005), 在北山东部形成白云山东七一山岛弧带, 西部形成窑洞努如-公婆泉岛弧带, 这也得到了一些年代学的印证, 如红柳河北与俯冲密切相关花岗岩的锆石 U-Pb 年龄分别为 441.4 ± 1.6 Ma 和 440.9 ± 1.3 Ma, 星星峡火山弧钙碱性花岗岩类的锆石 U-Pb 年龄为 424.9 ± 5.8 Ma(李伍平等, 2001; Lei *et al.*, 2011)。

目前, 尽管对北山地区的构造演化过程研究程度较低, 洋盆闭合时限仍存在较大争议, 但越来越多的证据表明该区古大洋在早泥盆世已闭合并进入后碰撞伸展阶段(张元元等, 2008; 李舢等, 2009; 王立社等, 2009; 王磊等, 2015)。红柳河-牛圈子-洗肠井蛇绿岩带所代表的古洋盆已于晚志留世末期闭合, 因此炭山子东橄榄辉长岩不可能是红柳河-牛圈子-洗肠井蛇绿岩所代表的古洋盆南向俯冲过程中的产物。而形成于活动大陆边缘弧的炭山子东橄榄辉长岩(366.0 ± 2.8 Ma)指示在晚泥盆世晚期北山地区还存在残留洋盆或弧后盆地的洋壳发生了再次俯冲作用。从区域地质背景来看, 在炭山子东橄榄辉长岩南部分布有辉铜山-帐房山蛇绿岩带(SSZ 型), 其中辉长岩 LA-ICP-MS 锆石 U-Pb 年分别为 446.1 ± 3.0 Ma、 362.1 ± 4.0 Ma(余吉远等, 2012; 王国强, 2015), 指示辉铜山-帐房山蛇绿岩所代表的弧后盆地从晚志留世-早石炭世持续存在。因此, 本文认为炭山子东橄榄辉长岩的形成与辉铜山-帐房山蛇绿岩所代表的弧后盆地的北向俯冲有关, 即其形成环境为活动大陆边缘弧。在俯冲作用过程中亏损岩石圈地幔在俯冲流体的作用下发生部分熔融, 在岩浆上升过程中发生过分离结晶作用, 最终侵位形成大山头-黑山一带的基性-超基性杂岩体, 局部伴有铜镍矿化。

另外, 在大山头-黑山一带及邻近地区发育大量与中晚泥盆世基性-超基性岩体形成时代相近的花岗岩类, 其 $\varepsilon\text{Nd}(t)$ 为 $-3.8 \sim +0.3$, 显示了幔源物质的贡献(王涛等, 2008; 李舢等, 2009), 这与东天山及中国东北红旗岭等地区的基性-超基性岩体与邻近的花岗岩类的形成时代相近的特征十分相似(Han *et al.*, 1997; Wu *et al.*, 2002)。韩宝福等(1998, 2004)认为中亚造山带在显生宙地壳生长过程中, 基性-超基性杂岩与邻近的花岗岩形成时代相近可能具有普遍意义, 可能与岩石圈地幔拆沉和软流圈地幔上涌、熔融作用密切相关, 可以作为幔源岩浆侵入

地壳导致地壳垂向生长的最直接的标志。因此,大山头-黑山一带基性-超基性杂岩体高精度锆石U-Pb年龄的获得,为中亚造山带地壳垂向生长提供了重要的岩石学和年代学证据。

7 结论

(1) 炭山子东橄榄辉长岩是辉铜山-帐房山蛇绿岩所代表的弧后盆地北向俯冲过程中受俯冲流体交代上覆岩石圈地幔发生部分熔融的产物,形成于活动大陆边缘。

(2) 炭山子东橄榄辉长岩 LA-ICP-MS 锆石 U-Pb 年龄为 366.0 ± 2.8 Ma, 为辉铜山-帐房山蛇绿岩所代表的弧后盆地北向俯冲进一步提供了年代学证据。

(3) 在大山头一带及其邻区发育大量与基性-超基性杂岩体形成时代相近的花岗岩类,这与岩石圈地幔拆沉和软流圈地幔上涌、熔融作用密切相关,可以作为幔源岩浆侵入地壳导致北山地区地壳垂向生长的最直接的证据。

References

- Bai Yunlai, Chen Qilin, Tang Zhongli, et al. 2004. The characteristics of basic-ultrabasic rocks in the back-arc rift system on the northeastern margin of the Tarim plate[J]. Geology in China, 31(3): 254~261 (in Chinese with English abstract).
- Condie K C. 1989. Geochemical changes in basalts and andesites across the Archean-Proterozoic boundary: Identification and significance[J]. Lithos, 23(1): 1~18.
- Dai Shuang, Fang Xiaomin, Zhang Xiang, et al. 2003. The origin and tectonic settings of diorite granitoid in the centre of Beishan region of Gansu[J]. Journal of Lanzhou University (Natural Sciences), 39(1): 86~92 (in Chinese with English abstract).
- Elliott T, Plank T, Zindler A, et al. 1997. Elements transport from slab to volcanic front the Mariana arc [J]. Journal of Geophysical Research, 102: 14 991~15 019.
- Fan Yuxin, Bai Yunlai, Zhang Mingjie, et al. 2003. Geochemical and petrological information and its implications for the ultramafic complex from Mazongshan Mountain in the western region of Gansu Province [J]. Journal of Lanzhou University (Natural Sciences), 29(4): 93~97 (in Chinese with English abstract).
- Gong Quansheng, Liu Mingqiang, Li Hailin, et al. 2002. The type and basic characteristics of Beishan orogenic belt, Gansu[J]. Northwestern Geology, 35(3): 28~34 (in Chinese with English abstract).
- Gong Quansheng, Liu Mingqiang, Liang Minghong, et al. 2003. The tectonic facies and tectonic evolution of Beishan orogenic belt, Gansu[J]. Northwestern Geology, 36(1): 11~19 (in Chinese with English abstract).
- Han Baofu, He Guoqi, Wang Shiguang, et al. 1998. Postcollisional mantle-derived magmatism and vertical growth of the continental crust in north Xinjiang[J]. Geological Review, 44(4): 396~406 (in Chinese with English abstract).
- Han Baofu, Ji Jianqing, Song Biao, et al. 2004. Shrimp zircon U-Pb age and its geological significance of the mafic ultramafic complex containing Cu Ni ore in karatongke and Huangshan, Xinjiang[J]. Science Bulletin, 49(22): 2 324~2 328 (in Chinese with English abstract).
- Han B F, Wang S G, Jahn B M, et al. 1997. Depleted-mantle source for the Ulungur River A-type granites from North Xinjiang, China: Geochemistry and Nd-Sr isotopic evidence, and implications for Phanerozoic crustal growth[J]. Chemical Geology, 138(3~4): 135~159.
- He Shiping, Ren Bingchen, Yao Wenguang, et al. 2002. The division of tectonic units of Beishan area, Gansu-Inner Mongolia[J]. Northwestern Geology, 35(4): 30~40 (in Chinese with English abstract).
- He Shiping, Zhou Huiwu, Ren Bingchen, et al. 2005. Crustal evolution of Palaeozoic in Beishan area, Gansu and Inner Mongolia, China[J]. Northwestern Geology, 38(3): 6~15 (in Chinese with English abstract).
- He Zhenyu, Zong Keqing, Jiang Hongying, et al. 2014. Early Paleozoic tectonic evolution of the southern Beishan orogenic collage: Insights from the granitoids[J]. Acta Petrologica Sinica, 30(8): 2 324~2 338 (in Chinese with English abstract).
- Hou Qingye, Wang Zhong, Liu Jinbao, et al. 2012. Geochemistry characteristics and SHRIMP dating of Yueyashan ophiolite in Beishan orogen[J]. Geoscience, 26(5): 1 008~1 018 (in Chinese with English abstract).
- Jahn B M, Wu F Y and Chen B. 2000. Granitoids of the central Asian orogenic belt and continental growth in the Phanerozoic[J]. Transactions of the Royal Society of Edinburgh: Earth Sciences, 91(1~2): 181~193.
- Jiang Changyi, Cheng Songlin, Ye Shufeng, et al. 2006. Lithogeochemistry and petrogenesis of Zhongposhanbei mafic rock body, at Beishan region, Xinjiang[J]. Acta Petrologica Sinica, 22(1): 115~126 (in Chinese with English abstract).
- La Flèche M R, Camiré G and Jenner G A. 1998. Geochemistry of post-

- Acadian, Carboniferous continental intraplate basalts from the Maritimes Basin, Magdalen Islands, Québec, Canada [J]. *Chemical Geology*, 148(3~4): 115~136.
- Lei R X, Wu C Z, Gu L X, et al. 2011. Zircon U-Pb chronology and Hf isotope of the Xingxingxia granodiorite from the Central Tianshan zone (NW China): Implications for the tectonic evolution of the southern Altaids [J]. *Gondwana Research*, 20: 582~593.
- Li Jinyi, Wang Kezhuo, Li Yaping, et al. 2006. Geomorphological features, crustal composition and geological evolution of Tianshan Mountains [J]. *Geological Bulletin of China*, 25(8): 895~909 (in Chinese with English abstract).
- Li Li, Wang Yuxi, Li Xing, et al. 2010a. A new structural type of basic-ultrabasic complex with Ni-Cu mineralization [J]. *Northwestern Geology*, 43(3): 47~55 (in Chinese with English abstract).
- Li Li, Yang Yongqiang and Wang Yuxi. 2010b. Geochemical characteristics and petrogenesis of Guaishishan copper-nickel mineralized mafic-ultramafic complex in Beishan region of Gansu [J]. *Global Geology*, 29(1): 18~27 (in Chinese with English abstract).
- Li Shan, Wang Tao, Tong Ying, et al. 2009. Identification of the Early Devonian Shuangfengshan A-type granites in Liuyuan area of Beishan and its implications to tectonic evolution [J]. *Acta Petrologica et Mineralogica*, 28(5): 407~422 (in Chinese with English abstract).
- Li Wuping, Wang Tao, Li Jinbao, et al. 2001. The U-Pb age of zircon from late Caledonian granitoids in Hongliuhe area, east Tianshan Mountains, northwest China and its geological implications [J]. *Acta Geoscientia Sinica*, 22(3): 231~235 (in Chinese with English abstract).
- Liang Xirong, Wei Gangjian, Li Xianhua, et al. 2003. Precise measurement of $^{143}\text{Nd}/^{144}\text{Nd}$ ratios using multiple-collectors inductively coupled plasma-mass spectrometer (MC-ICPMS) [J]. *Geochimica*, 32(1): 91~96 (in Chinese with English abstract).
- Liu Xueya and Wang Quan. 1995. Tectonics of orogenic belts in Beishan Mts, western China and their evolution [J]. *Geoscience Research*, 28: 37~48 (in Chinese with English abstract).
- Nie Fengjun, Jiang Sihong, Bai Daming, et al. 2002. Metallogenic Studies and Ore Prospecting in Conjunction Area of Inner Mongolia Autonomous Region, Gansu Province and Xinjiang Uygur Autonomous Region (Beishan Mt.), Northwest China [M]. Beijing: Geological Publishing House, 1~408 (in Chinese with English abstract).
- Pearce J A, Lippard S J, Lippard S J, et al. 1984. Characteristics and tectonic significance of super-subduction zone ophiolite [A]. Kokelaar B P and Howells M F. *Marginal Basin Geology* [C]. Geological Society, London, Special Publications, 16(1): 77~94.
- Rickwood P C. 1989. Boundary lines within petrologic diagrams which use oxides for major and minor element [J]. *Lithos*, 22: 246~263.
- Sengör A M C, Natal' In B A and Burtman V S. 1993. Evolution of the Altaiid tectonic collage and Palaeozoic crustal growth in Eurasia [J]. *Nature*, 364(6435): 299~307.
- Shao Xiaoyang, Sun Bainian, Li Xiangchuan, et al. 2010. Geological features and metallogenesis of Heishan copper-nickel deposit in Subei county of Gansu Province [J]. *Gansu Geology*, 19(3): 19~25 (in Chinese with English abstract).
- Song D F, Xiao W J, Han C M, et al. 2013a. Provenance of metasedimentary rocks from the Beishan orogenic collage, southern Altaids: Constraints from detrital zircon U-Pb and Hf isotopic data [J]. *Gondwana Research*, 24(3~4): 1127~1151.
- Song D F, Xiao W J, Han C M, et al. 2013b. Progressive accretionary tectonics of the Beishan orogenic collage, southern Altaids: Insights from zircon U-Pb and Hf isotopic data of high-grade complexes [J]. *Precambrian Research*, 227: 368~388.
- Sun S S and McDonough W F. 1989. Chemical and isotopic systems of oceanic basalts: Implications for Mantle composition and processes [J]. Geological Society, London, Special Publications, 42(1): 313~345.
- Tian Z H, Xiao W J, Windley B F, et al. 2014. Structure, age, and tectonic development of the Huoshishan-Niujuanzhi ophiolitic mélange, Beishan, southernmost Altaids [J]. *Gondwana Research*, 25(2): 820~841.
- Wang Guoqiang. 2015. Paleozoic Ophiolite and Volcanic Rocks in Beishan and their Tectonic Evolution [D]. Xi'an: Chang'an University (in Chinese).
- Wang Lei, Yang Jianguo, Wang Xiaohong, et al. 2013. Comparison of geochemistry characteristics and analysis on the metallogenic potential of ultrabasic rocks in Shijintan of Beishan area, Gansu Province [J]. *Xinjiang Geology*, 31(1): 65~70 (in Chinese with English abstract).
- Wang Lei, Yang Jianguo, Wang Xiaohong, et al. 2015. LA-ICP-MS zircon U-Pb dating and its geological implications of Yingmaotuo granitic rocks [J]. *Bulletin of Mineralogy, Petrology and Geochemistry*, 34(3): 583~591 (in Chinese with English abstract).
- Wang Lishe, Yang Jianguo, Xie Chunlin, et al. 2007. The discovery and geological significance of an early Paleozoic ophiolite mélange belt in the Huoshishan part of Beishan Mountain, Gansu Province, China [J]. *Geoscience*, 21(3): 451~456 (in Chinese with English abstract).
- Wang Lishe, Yang Jianguo, Xie Chunlin, et al. 2008. Metallogenic po-

- tentiality of Guanshishan Cu-Ni mineralized basic-ultrabasic rocks in Beishan area Gansu Province [J]. *Geotectonica et Metallogenica*, 32(3): 392~399 (in Chinese with English abstract).
- Wang Lishe, Yang Jianguo, Xie Chunlin, et al. 2009. Geochronology and geochemistry of Haergentoukoubu granites in the Beishan area, Gansu, China and their geological significance [J]. *Acta Geologica Sinica*, 83(3): 377~387 (in Chinese with English abstract).
- Wang Tao, Li Wuping, Li Jinbao, et al. 2008. Increase of juvenile mantle-derived composition from syn-orogenic to post-orogenic granites of the east part of the eastern Tianshan (China) and implications for continental vertical growth: Sr and Nb isotopic evidence [J]. *Acta Petrologica Sinica*, 24(4): 762~772 (in Chinese with English abstract).
- Wei Gangjian, Liang Xirong, Li Xianhua, et al. 2002. Precise measurement of Sr composition of liquid and solid base using (LP) MC-ICPMS [J]. *Geochimica*, 31(3): 295~299 (in Chinese with English abstract).
- Wiedenbeck M, Alle P, Corfu F, et al. 1995. Three natural zircon standards for U-Th-Pb, Lu-Hf, trace element and REE analyses [J]. *Geost. and Newsl.*, 19: 1~23.
- Wilson M. 1989. Igneous Petrogenesis [M]. London: Unwin Hyman, 1~466.
- Windley B F, Alexeiev D, Xiao W J, et al. 2007. Tectonic models for accretion of the Central Asian Orogenic Belt [J]. *Journal of the Geological Society*, 164(1): 31~47.
- Wood D A, Joron J L and Treuil M. 1979. A re-appraisal of the use of trace elements to classify and discriminate between Mag Ma series erupted in different tectonic settings [J]. *Earth and Planetary Science Letters*, 45(2): 326~336.
- Wu F Y, Sun D Y, Li H M, et al. 2002. A-type granites in northeastern China: Age and geochemical constraints on their petrogenesis [J]. *Chemical Geology*, 187(1~2): 143~173.
- Wu Peng, Wang Guoqiang, Li Xiangmin, et al. 2012. The age of Niujuanzi ophiolite in Beishan area of Gansu Province and its geological significance [J]. *Geological Bulletin of China*, 31(12): 2 032~2 037 (in Chinese with English abstract).
- Xiao W J, Mao Q G, Windley B F, et al. 2010. Paleozoic multiple accretionary and collisional processes of the Beishan orogenic collage [J]. *American Journal of Science*, 310(10): 1 553~1 594.
- Xiao W J, Zhang L C, Qin K Z, et al. 2004. Paleozoic accretionary and collisional tectonics of the eastern Tianshan (China): Implications for the continental growth of Central Asia [J]. *American Journal of Science*, 304(4): 370~395.
- Xie W, Song X Y, Deng Y F, et al. 2012. Geochemistry and petrogenetic implications of a Late Devonian mafic-ultramafic intrusion at the southern margin of the Central Asian Orogenic Belt [J]. *Lithos*, 144~145: 209~230.
- Xie Wei, Song Xieyan, Deng Yufeng, et al. 2013. Geology and olivine geochemistry of the Heishan Ni-Cu-(PGE) sulfide deposit, Gansu, NW China [J]. *Acta Petrologica Sinica*, 29(10): 3 487~3 502 (in Chinese with English abstract).
- Xie Xie, Yang Jianguo, Wang Xiaohong, et al. 2013. The geology, geochemical characteristics and metallogenetic potential of Dashantou Cu-Ni mineralized mafic-ultramafic rocks in Beishan, Gansu Province [J]. *Xinjiang Geology*, 31(4): 353~359 (in Chinese with English abstract).
- Xie Xie, Yang Jianguo, Wang Xiaohong, et al. 2015. Zircon SHRIMP U-Pb dating of Hongliugou mafic-ultramafic complex in the Beishan area of Gansu Province and its geological significance [J]. *Geology in China*, 42(2): 396~405 (in Chinese with English abstract).
- Xu Gang, Tang Zhongli, Wang Yalei, et al. 2012. Features and genetic significance of olivine from Heishan magmatic sulfide ore-bearing intrusion in Beishan area, Gansu Province [J]. *Mineral Deposits*, 31(5): 1 075~1 086 (in Chinese with English abstract).
- Yan Haiqing, Zhao Huanqiang, Ding Ruiying, et al. 2012. Zircon SHRIMP U-Pb dating of the Dashantou basic complex and its geological significance in Beishan area, Gansu Province [J]. *Northwestern Geology*, 45(4): 216~228 (in Chinese with English abstract).
- Yang Hequn, Li Ying, Zhao Guobin, et al. 2010. Character and structural attribute of the Beishan ophiolite [J]. *Northwestern Geology*, 43(1): 26~36 (in Chinese with English abstract).
- Yang Jianguo, Wang Lei, Wang Xiaohong, et al. 2012. Zircon SHRIMP U-Pb dating of Heishan mafic-ultramafic complex in the Beishan area of Gansu Province and its geological significance [J]. *Geological Bulletin of China*, 31(2~3): 448~454 (in Chinese with English abstract).
- Yu Fusheng, Wang Chunying, Qi Jiafu, et al. 2000. The clarification and tectonic implication of the early Silurian ophiolite melange in Hongliuhe area [J]. *Mineral Petrology*, 20(4): 60~66 (in Chinese with English abstract).
- Yu Jiyuan, Li Xiangmin, Wang Guoqiang, et al. 2012. Zircon U-Pb ages of Huitongshan and Zhangfangshan ophiolite in Beishan of Gansu-Inner Mongolia border area and their significance [J]. *Geological Bulletin of China*, 31(12): 2 038~2 045 (in Chinese with English abstract).
- Yuan H L, Gao S, Liu X M, et al. 2004. Accurate U-Pb age and trace element determinations of zircon by laser ablation-inductively coupled

- plasma-mass spectrometry [J]. *Geostandards and Geoanalytical Research*, 28(3): 353~370.
- Zhang Xinhui, Feng Jun, Yin Yong, et al. 2012. Comparative study on the characteristic occurrences of Heishan Ni-Cu deposit in Subei County of Gansu Province [J]. *Northwestern Geology*, 45(4): 134~144 (in Chinese with English abstract).
- Zhang Yuanyuan and Guo Zhaojie. 2008. Accurate constraint on formation and emplacement age of Hongliuhe ophiolite, boundary region between Xinjiang and Gansu Provinces and its tectonic implications [J]. *Acta Petrologica Sinica*, 24(4): 803~809 (in Chinese with English abstract).
- Zheng Rongguo, Wu Tairan, Zhang Wen, et al. 2012. Geochemical characteristics and tectonic setting and of the Yueyashan-Xichangjing ophiolite in the Beishan area [J]. *Acta Geologica Sinica*, 86(6): 961~971 (in Chinese with English abstract).
- Zindler A and Hart S R. 1986. Chemical geodynamics [J]. *Ann. Rev. Earth Plant. Sci.*, 14: 493~571.
- Zuo Guochao, Li Maosong, et al. 1996. Formation and Evolution of Early Paleozoic Lithosphere of Beishan Region, West Gansu [M]. Science and Technical Press of Gansu Province, 1~93 (in Chinese with English abstract).
- Zuo Guochao, Liu Yike and Liu Chunyan. 2003. Framework and evolution of the tectonic structure in Beishan area across Gansu Province, Xinjiang Autonomous Region and Inner Mongolia Autonomous Region [J]. *Acta Geologica Gansu*, 1(12): 1~15 (in Chinese with English abstract).
- 与陆壳纵向生长 [J]. *地质论评*, 44(4): 396~406.
- 韩宝福,季建清,宋彪,等.2004.新疆喀拉通克和黄山东含铜镍矿镁铁-超镁铁杂岩体的SHRIMP锆石U-Pb年龄及其地质意义 [J].*科学通报*, 49(22): 2324~2328.
- 何世平,任秉琛,姚文光,等.2002.甘肃内蒙古北山地区构造单元划分 [J].*西北地质*, 35(4): 30~40.
- 何世平,周会武,任秉琛,等.2005.甘肃内蒙古北山地区古生代地壳演化 [J].*西北地质*, 38(3): 6~15.
- 贺振宇,宗克清,姜洪颖,等.2014.北山造山带南部早古生代构造演化:来自花岗岩的约束 [J].*岩石学报*, 30(8): 2324~2338.
- 侯青叶,王忠,刘金宝,等.2012.北山月牙山蛇绿岩地球化学特征及SHRIMP定年 [J].*现代地质*, 26(5): 1008~1018.
- 姜常义,程松林,叶书锋,等.2006.新疆北山地区中坡山北镁铁质岩体岩石地球化学与岩石成因 [J].*岩石学报*, 22(1): 115~126.
- 李锦铁,王克卓,李亚平,等.2006.天山山脉地貌特征、地壳组成与地质演化 [J].*地质通报*, 25(8): 895~909.
- 李丽,王育习,李行,等.2010a.一种新构造类型的含铜镍矿化基性-超基性杂岩体 [J].*西北地质*, 43(3): 47~55.
- 李丽,杨永强,王育习.2010b.甘肃北山地区怪石山古铜镍矿化镁铁质-超镁铁质杂岩体的地球化学特征及成因机制 [J].*世界地质*, 29(1): 18~27.
- 李舢,王涛,童英,等.2009.北山柳园地区双峰山早泥盆世A型花岗岩的确定及其构造演化意义 [J].*岩石矿物学杂志*, 28(5): 407~422.
- 李伍平,王涛,李金宝,等.2001.东天山红柳河地区晚加里东期花岗岩类岩石锆石U-Pb年龄及其地质意义 [J].*地球学报*, 22(3): 231~235.
- 梁细荣,韦刚健,李献华,等.2003.利用MC-ICPMS精确测定¹⁴³Nd/¹⁴⁴Nd和Sm/Nd比值 [J].*地球化学*, 32(1): 91~96.
- 刘雪亚,王荃.1995.中国西部北山造山带的大地构造及其演化 [J].*地学研究*, 28: 37~48.
- 聂凤军,江思宏,白大明,等.2002.北山地区金属矿床成矿规律及找矿方向 [M].北京:地质出版社, 1~408.
- 邵小阳,孙柏年,李相传,等.2010.甘肃肃北黑山铜镍矿成矿地质特征及成因探讨 [J].*甘肃地质*, 19(3): 19~25.
- 王国强.2015.北山古生代蛇绿岩、火山岩研究与构造演化 [D].西安:长安大学.
- 王磊,杨建国,王小红,等.2013.甘肃北山拾金滩岩体与邻区超基性岩体岩石地球化学特征对比及成矿潜力浅析 [J].*新疆地质*, 31(1): 65~70.
- 王磊,杨建国,王小红,等.2015.甘肃北山营毛沱地区花岗岩类LA-ICP-MS锆石U-Pb定年及地质意义 [J].*矿物岩石地球化学*

附中文参考文献

- 白云来,陈启林,汤中立,等.2004.塔里木板块东北边缘弧后裂谷系统基性-超基性岩特征 [J].*中国地质*, 31(3): 254~261.
- 戴霜,方小敏,张翔,等.2003.北山中部地区闪长岩-花岗岩类成因及构造背景 [J].*兰州大学学报(自然科学版)*, 39(1): 86~92.
- 范育新,白云来,张铭杰,等.2003.甘肃西部马鬃山超镁铁质杂岩岩石学地球化学信息及意义 [J].*兰州大学学报(自然科学版)*, 29(4): 93~97.
- 龚全胜,刘明强,李海林,等.2002.北山造山带类型及基本特征 [J].*西北地质*, 35(3): 28~34.
- 龚全胜,刘明强,梁明宏,等.2003.北山造山带大地构造相机构造演化 [J].*西北地质*, 36(1): 11~19.
- 韩宝福,何国琦,王世洸,等.1998.新疆北部后碰撞幔源岩浆活动

- 通报, 34(3): 583~591.
- 王立社, 杨建国, 谢春林, 等. 2007. 甘肃北山火石山地区早古生代蛇绿混杂岩的发现及其地质意义[J]. 现代地质, 21(3): 451~456.
- 王立社, 杨建国, 谢春林, 等. 2008. 甘肃怪石山铜镍矿化基性超基性岩成矿潜力研究[J]. 大地构造与成矿学, 32(3): 392~399.
- 王立社, 杨建国, 谢春林, 等. 2009. 甘肃北山火石山哈尔根头口布花岗岩年代学、地球化学及其地质意义[J]. 地质学报, 83(3): 377~387.
- 王 涛, 李伍平, 李金宝, 等. 2008. 东天山东段同造山到后造山花岗岩幔源组分的递增及陆壳垂向生长意义——Sr、Nd 同位素证据[J]. 岩石学报, 24(4): 762~772.
- 韦刚健, 梁细荣, 李献华, 等. 2002. (LP) MC-ICPMS 方法精确测定液体和固体样品的 Sr 同位素组成[J]. 地球化学, 31(3): 295~299.
- 武 鹏, 王国强, 李向民, 等. 2012. 甘肃北山地区牛圈子蛇绿岩的形成时代及地质意义[J]. 地质通报, 31(12): 2 032~2 037.
- 颉 炜, 宋谢炎, 邓宇峰, 等. 2013. 甘肃黑山铜镍硫化物含矿岩体的地质特征及橄榄石成因探讨[J]. 岩石学报, 29(10): 3 487~3 502.
- 谢 燮, 杨建国, 王小红, 等. 2013. 甘肃北山大山头一带铜镍矿化基性-超基性岩地质、地球化学特征及成矿潜力[J]. 新疆地质, 31(4): 353~359.
- 谢 燮, 杨建国, 王小红, 等. 2015. 甘肃北山红柳沟铜镍矿化基性-超基性岩体 SHRIMP 镆石 U-Pb 年龄及其地质意义[J]. 中国地质, 42(2): 396~405.
- 徐 刚, 汤中立, 王亚磊, 等. 2012. 甘肃北山黑山岩浆铜镍硫化物矿床橄榄石特征及成因意义[J]. 矿床地质, 31(5): 1 075~1 086.
- 闫海卿, 赵换强, 丁瑞颖, 等. 2012. 甘肃北山大山头基性杂岩体 SHRIMP 镆石 U-Pb 年龄及其地质意义[J]. 西北地质, 45(4): 216~228.
- 杨合群, 李 英, 赵国斌, 等. 2010. 北山蛇绿岩特征及构造属性[J]. 西北地质, 43(1): 26~36.
- 杨建国, 王 磊, 王小红, 等. 2012. 甘肃北山地区黑山铜镍矿化基性-超基性杂岩体 SHRIMP 镆石 U-Pb 定年及其地质意义[J]. 地质通报, 31(2~3): 448~454.
- 于福生, 王春英, 漆家福, 等. 2000. 甘新交界红柳河地区早志留世蛇绿混杂岩的厘定及大地构造意义[J]. 矿物岩石, 20(4): 60~66.
- 余吉远, 李向民, 王国强, 等. 2012. 甘肃北山地区辉铜山和帐房山蛇绿岩 LA-ICP-MS 镆石 U-Pb 年龄及地质意义[J]. 地质通报, 31(12): 2 038~2 045.
- 张新虎, 冯 军, 殷 勇, 等. 2012. 甘肃肃北黑山镍铜矿床产出特征及对比研究[J]. 西北地质, 45(4): 134~144.
- 张元元, 郭召杰. 2008. 甘新交界红柳河蛇绿岩形成和侵位年龄的准确限定及大地构造意义[J]. 岩石学报, 24(4): 803~809.
- 郑荣国, 吴泰然, 张 文, 等. 2012. 北山地区月牙山-洗肠井蛇绿岩的地球化学特征及形成环境[J]. 地质学报, 86(6): 961~971.
- 左国朝, 李茂松, 等. 1996. 甘肃北山地区早古生代岩石圈形成与演化[M]. 兰州: 兰州甘肃科技出版社, 1~93.
- 左国朝, 刘义科, 刘春燕. 2003. 甘新蒙北山地区构造格局及演化[J]. 甘肃地质学报, 1(12): 1~15.